Received: 13 April 2020 | Revised: 17 June 2020 | Accepted: 3 August 2020

DOI: 10.4218/etrij.2020-0158

ORIGINAL ARTICLE

ETRI Journal WILEY

Reduction of sidelobe levels in multicarrier radar signals via the fusion of hill patterns and geometric progression

Channapatna Gopalkrishna Raghavendra | **Raghu Srivatsa Marasandra Prakash** | **Vignesh Nayak Panemangalore**

Department of Electronics and Communication, Ramaiah Institute of Technology, Bangalore, Karnataka, India

Correspondence
Channapatna Gopalkrishna Raghavendra, Department of Electronics and Communication, Ramaiah Institute of Technology, Bangalore, Karnataka, India.
Email: cgraagu@msrit.edu

Multi-carrier waveforms have several advantages over single-carrier waveforms for radar communication. Employing multi-carrier complementary phase-coded (MCPC) waveforms in radar applications has recently attracted significant attention. MCPC radar signals take advantage of orthogonal frequency division multiplexing properties, and several authors have explored the use of MCPC signals and the difficulties associated with their implementation. The sidelobe level and peak-to-mean-envelope-power ratio (PMEPR) are the key issues that must be addressed to improve the performance of radar signals. We propose a scheme that applies pattern-based scaling and geometric progression methods to enhance sidelobe and PMEPR levels in MCPC radar signals. Numerical results demonstrate the improvement of sidelobe and PMEPR levels in the proposed scheme. Additionally, autocorrelations are obtained and analyzed by applying the proposed scheme in extensive simulation experiments.

KEYWORDS
Differential geometric progression, MCPC, OFDM, PMEPR, sidelobe level, TSSWA

1 | INTRODUCTION

Bandwidth is a key concept in radio communications, which should be utilized efficiently. There is a huge demand for bandwidth in radar communications if single-carrier modulation schemes are adopted. The concept of orthogonal frequency division multiplexing (OFDM) can be utilized for the transmission of the radar signals to reduce bandwidth requirements [1]. Recently, there has been rapid growth in multimedia wireless applications based on an increase in multimedia traffic. Significant research has focused on the development of innovative technology to improve data transmission rates. Similarly, in the area of radar communications, there is a need for novel approaches to balance the trade-off between range and resolution. The most significant features of radar signals are their range and resolution. The range of a radar signal can be improved by increasing the pulse width, but this technique reduces the resolution. Therefore, to improve the resolution, pulse width must be reduced. To balance range and resolution, it has been suggested to apply the pulse compression technique [2]. Pulse compression takes advantage of the best features of both long and short-duration pulses and facilitates the use of long waveforms to obtain high energy while simultaneously matching the resolution of a short pulse via the internal modulation of a long pulse.

Levanon [3] defined the concept of multicarrier complementary phase-coded (MCPC) signals. Digital phase coding

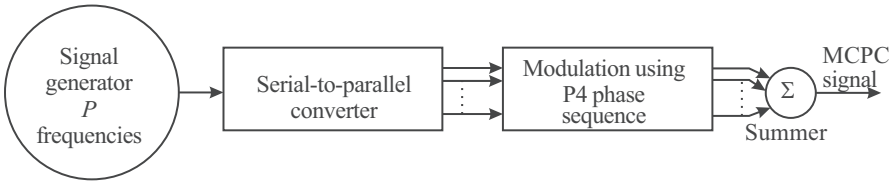

FIGURE 1 Schematic of an OFDM signal generator

as a means of internal modulation was used to develop MCPC signals. However, MCPC signals have a poor peak-to-mean-envelope-power ratio (PMEPR). In [4], various techniques were used to improve PMEPR levels, but sidelobe levels were not improved significantly. If efforts are made to reduce PMEPR values, then sidelobe levels increase and vice versa. Therefore, there is a need to balance PMEPR and sidelobe levels.

Several researchers have conducted investigations and experiments to curtail the impact of PMEPR on OFDM signals. The majority of these works have focused on data transmission applications, such as novel adaptive tone reservation methods [5], improved tone reservation schemes with fast convergence [6], and signal-to-clipping-noise-ratio-based tone reservation methods [7]. A number of researchers have analyzed the reduction in PMEPR values in multicarrier signals for radar functions. In [8], a phase modulation method was proposed. An iterative least-squares method was used in [9]. A genetic algorithm approach was presented in [10], and a random phase updating algorithm was adopted in [11]. For condensing sidelobes, experiments were conducted using a constellation adjustment technique in [12]. Li et al. [13] proposed a sequential quadratic programming technique and genetic algorithm to reduce sidelobe levels, but this method results in poor computational efficiency. The Broyden–Fletcher–Goldfarb–Shanno method was adopted in [14]. All of the studies mentioned focused on reducing either PMPER or sidelobe levels separately. A few researchers have investigated the joint reduction of these issues [15–17], but their solutions are limited to non-radar applications. In [18], the Zadoff-Chu sequence and a signal cancellation method were applied to reduce autocorrelation sidelobe levels and maintain a low PMEPR. Improvements of 0.7075 in terms of the PMEPR and 3.28 dB in terms of the sidelobe level were achieved, but this system is limited to five carriers. This paper proposes a novel algorithm to develop multicarrier radar signals by fusing hill patterns and geometric progression methods to reduce both PMEPR and sidelobe levels for large numbers of carriers with various sequence orderings.

The remainder of this paper is organized as follows. In Section II, MCPC signal implementation is illustrated. In Section III, the two-sample sliding window adder (TSSWA) method is discussed. Section IV discusses subcarrier weighting in MCPC signals. Section V proposes the development of MCPC signals based on a differential geometric progression technique. Section VI presents comparisons and detailed discussions. Section VII summarizes our conclusions based on experimental results.

2 | CHARACTERISTICS OF MCPC SIGNALS

MCPC radar signals are developed based on the concept of an OFDM scheme. MCPC radar signals are composed of N subcarriers that are all transmitted in parallel with a frequency spacing of t_c which yields an OFDM signal. The concept of transmitting all orthogonal subcarriers is well-known in the communications field. MCPC radar signals are implemented by modulating the phases of orthogonal subcarriers using polyphase codes, called P3 and P4. The schematic is shown in Figure 1 for developing the MCPC radar signal.

MCPC signals are developed based on the cyclic shifts of P4 sequences. The phases for a P4 [2] digital phase modulation scheme with N phases are defined in (1).

$$\phi_n = \frac{\pi}{N}(n-1)(n-N-1) \quad \text{where } n = 1,\ 2,\ 3,\ \ldots,\ N. \tag{1}$$

This phase coding scheme contains a small number of phase values exhibiting ideal periodic thumbtack autocorrelation functions with peaky mainlobes and zero sidelobes.

The complex envelope of an MCPC OFDM signal is defined by (2).

$$s(t) = \sum_{v=1}^{N}\left[\sum_{u=1}^{N}\exp\left(j\phi_{u,v}\right)\exp\left\{j\left[2\pi f_s t\left(\frac{N+1}{2}-u\right)\right]\right\}\right] \underset{x[t-(v-1)t_c]}{} \tag{2}$$

$$\text{where } x(t) = \begin{cases} 1 & \text{if } 0 \le t \le t_c, \\ 0 & \text{otherwise.} \end{cases} \tag{3}$$

There are N subcarriers and N phase modulation chips, wheres t_c is the duration of each chip. The term $\exp\left\{j\left[2\pi f_s t(N+1/2-u)\right]\right\}$ in (2) corresponds to the subcarrier u. The term $\exp\left(j\phi_{u,v}\right)$ represents the vth element of the uth sequence modulating subcarrier u. This term mainly depends on v. When $v = 1$, it represents the unit pulse in the first chip duration. Similarly, when $v = N$, it represents the unit pulse in the Nth chip duration. $\phi_{u,v}$ denotes the vth

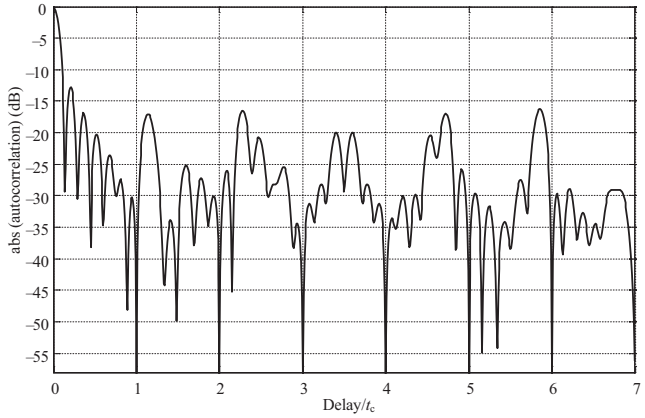

FIGURE 2 Autocorrelation function of a 7 × 7 MCPC signal for the ordering 1 234 567

phase element of the uth sequence. The term f_s denotes the frequency separation between any two adjacent subcarriers.

In an MCPC signal, N sequences are transmitted through N subcarriers and each sequence contains N phase-modulated chips. Therefore, N different subcarriers are modulated by N different phase sequences of length N. The frequency separation between any two consecutive subcarriers is the reciprocal of the chip duration, which defines an OFDM signal. The defining feature of such signals is pulse-to-pulse diversity (ie, each pulse is complementary to the other pulses). Additionally, this type of signal provides high spectral efficiency because the power spectrum is approximately rectangular with a spectral width of $N/2t_c$ and the average sidelobe level is 22.56 dB for P4-based 5 × 5 MCPC signals.

A 7 × 7 MCPC signal is considered with a phase sequence ordering of 1 234 567, which yields the minimum PMEPR. For a 7 × 7 MCPC signal, a total of 7! = 5040 orderings are possible, but the smallest PMEPR is obtained for continuous orderings of phase sequences, such as 1 234 567, 2 345 671, and 7 123 456. Signals with smaller PMEPR values provide larger sidelobe levels for autocorrelation, as shown in Figure 2, which results in poor detection performance. Signals with high PMEPR values provide small sidelobe levels. A reduction in PMEPR can be observed for the sequence ordering 1 234 567. Therefore, there is a trade-off between PMEPR and sidelobe levels.

3 | MCPC BASED ON THE TSSWA ALGORITHM

Lewis [19] proposed the TSSWA as a technique for reducing sidelobe levels using polyphase codes of type P1 and P4. In [20,21], the TSSWA technique was applied to individual carriers to reduce peak sidelobe levels. Here, we attempt to utilize a similar approach to reduce sidelobe levels in multicarrier signals.

Figure 3 presents a schematic of a TSSWA. The input signal for the TSSWA is divided into two basic operations. The first is to apply an autocorrelation function to the signal and the second is to delay the signal by t_c. This delay operation is performed in two sub-stages, each with a delay of t_c. The resulting signal yields reduced sidelobe levels that can be observed in simulation results.

Figure 4 presents the results of MCPC signals after applying the TSSWA technique to three, five, seven, and nine carriers. One can see that the sidelobe levels are significantly reduced.

Table 1 compares the signal levels of MCPC signals based on P4 polyphase codes and the TSSWA method for three, five, seven, and nine carriers. In a TSSWA, operations are not performed on the complex envelopes of MCPC signals. Instead, manipulation is applied directly to the autocorrelation functions of MCPC signals to obtain a clearer distinction between the mainlobe and sidelobes. Therefore, this algorithm does not have an impact on PMEPR levels. One can see an improvement in the sidelobe levels of MCPC signals based on the TWSSA compared with P4. Therefore, there is the potential to improve the balance between PMEPR and sidelobe levels in multicarrier signals.

4 | MCPC BASED ON SUBCARRIER WEIGHTING

Subcarrier weighting [22] is another technique that is used to suppress the sidelobe levels of OFDM systems. In this algorithm, simple scaling is performed on the subcarriers of OFDM signals. The scaling factors are selected in such a manner that sidelobes are controlled. With a few modifications, this principle can be applied to MCPC signals to improve the levels of PMEPR and sidelobes.

In (2), the subcarriers are modulated by digitally coded phases and a unit factor is selected for scaling. This equation can be modified by including the term w, which is a weighting coefficient that is used to scale every subcarrier in an MCPC signal. The corresponding modified equation is shown in (4).

$$s(t) = \sum_{v=1}^{N} \sum_{u=1}^{N} \exp\left(j\phi_{u,v}\right) w(u) \exp\left\{j\left[2\pi f_s t\right]\left(\frac{N+1}{2} - u\right)\right\} x\left[t - (v-1)\,t_c\right]. \quad (4)$$

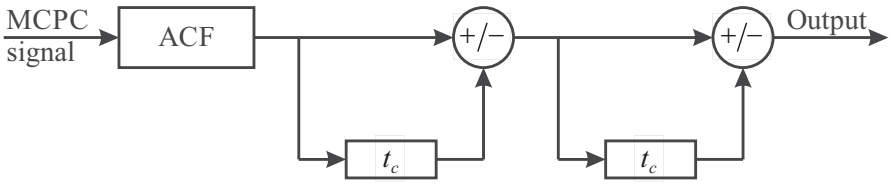

FIGURE 3 Block diagram of a TSSWA

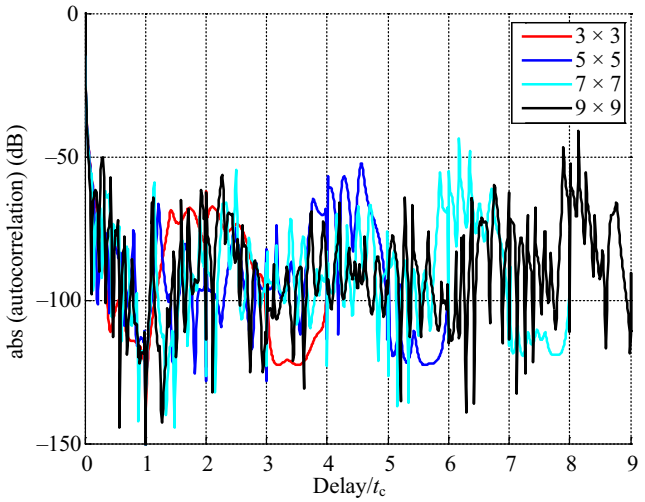

FIGURE 4 MCPC signals based on the TSSWA technique for 3 × 3, 5 × 5, 7 × 7 and 9 × 9 carriers

TABLE 1 Comparison of sidelobe levels of MCPC signals based on P4 and the TSSWA method

Carriers	SL (in dB) (P4-based)	SL (in dB) (TSSWA-based)
3 × 3	10.44	67.56
5 × 5	13.70	52.37
7 × 7	12.78	43.53
9 × 9	12.96	40.89

Here, an $N \times N$ MCPC signal is considered and the subcarrier weighting concept is applied. Each subcarrier is assigned a specific frequency associated with a weight, as shown in Figure 5. The subcarrier weighting is modified to achieve distinctive asymmetric weighting, pattern-based weighting, and differential geometric progression weighting.

4.1 | Distinctive asymmetric weighting (DSW)

DSW was developed based on subcarrier weighting, as shown in Figure 6. The weighting coefficients are obtained from the ratio of the maximum weight $g_{\max}$ to the minimum weight $g_{\min}$ and denoted by R such that the weight corresponding to one subcarrier is distinct from the weights of other subcarriers. In Figure 6, one can see that there is no symmetry of subcarrier frequency components about the zero frequency, which is also observed in P4-based MCPC signals. The weights corresponding to each subcarrier are calculated from g_1 to g_N with a step size of $X = (g_{\max} - g_{\min})/(N-1)$ for an $N \times N$ MCPC signal. The weights are normalized by dividing each weight by $g_{\max}$. Therefore, the weights assigned to different frequencies form the shape of a ramp.

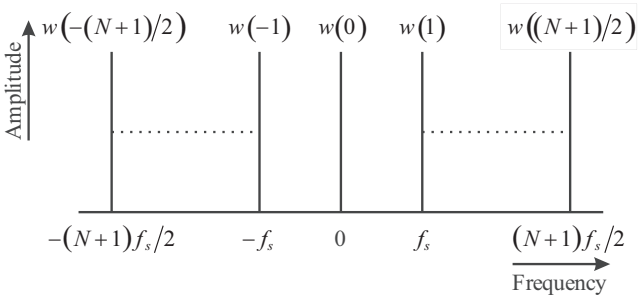

FIGURE 5 Subcarrier weighting

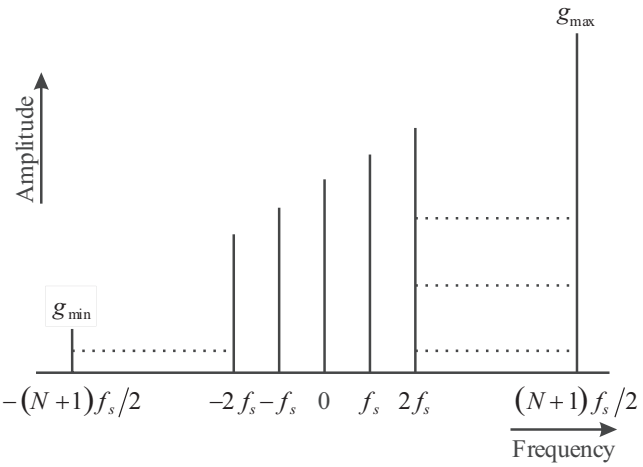

FIGURE 6 DSW

TABLE 2 Sidelobe and PMPER levels of a 5 × 5 MCPC signal based on DSW for the sequence ordering 12 345

R	SL (in dB)	PMEPR
$\sqrt{2}$	13.65	2.0274
$\sqrt{3}$	14.16	2.0760
$\sqrt{4}$	14.07	2.0873
$\sqrt{5}$	14.16	2.0980
$\sqrt{6}$	13.55	2.1040
$\sqrt{7}$	13.52	2.1072
$\sqrt{8}$	13.27	2.1088
$\sqrt{9}$	13.07	2.1093
$\sqrt{10}$	12.94	2.1092

In Table 2, one can see that the proposed weighting scheme yields favorable results for random values of R. $R = \sqrt{5}$ yields a desirable sidelobe level reduction for a 5 × 5 MCPC signal. However, enhanced results are not obtained in the cases of 7 × 7 and 9 × 9 MCPC signals for the same value of R. These results indicate that favorable ratios need not be deterministic. This finding motivated us to focus on further improvement.

4.2 | Pattern-based symmetric weighting (PBSW)

The DSW technique was developed for multicarrier radar signals in Section 4.1. This method can be extended to derive the PBSW technique from the original subcarrier weighting scheme. In PBSW, subcarrier scaling is performed by maintaining the symmetry of subcarrier weights. By performing scaling on subcarriers, four variants of symmetric patterns were developed. These variants are called the hill, valley, W, and M patterns. Weights are selected to scale the subcarrier frequencies such that these symmetric patterns can be obtained. These four symmetric pattern variants can be obtained if $w(u)$ in (4) is modified to $w(u) = w((N + 1/2) - u)$.

Figure 7A presents the hill pattern, where the weights of each subcarrier are modified such that they follow the shape of a hill. The weights increase from the far end of the zero frequency toward the near end on either side. Figure 7B presents the valley pattern, where the weights of each subcarrier are generated such that they all follow the pattern of a V. The weights decrease from the far end of the zero frequency toward the near end on either side. Figure 7C presents the M pattern, where the weights of each subcarrier are designed such that they follow the pattern of an M. Figure 7D presents the W pattern, where the weights of each subcarrier are designed such that they follow the pattern of a W.

Table 3 presents the results for the sidelobe and PMEPR levels of MCPC signals developed based on the PBSW method for five subcarriers with a sequence ordering of 12 345 and weighting factors of w_1 to w_5. One can see that a reduction in sidelobe levels only occurs in the case of weighting based on the hill pattern. Compared to the hill pattern, the valley pattern yields much worse results. In the other two cases, no significant changes can be observed in terms of sidelobe levels.

4.3 | Weighting based on a raised cosine pattern

The results obtained from hill-pattern-based weighting indicate that the reduction of sidelobe levels is possible only when the weight coefficients decrease symmetrically from the zero frequency on both sides. A raised cosine function follows a similar pattern, and there are many windows whose coefficients follow the pattern of a raised cosine, including Hamming, Hanning, Blackman, and Kaiser windows. Here, we attempt to develop an MCPC signal based on a raised cosine pattern.

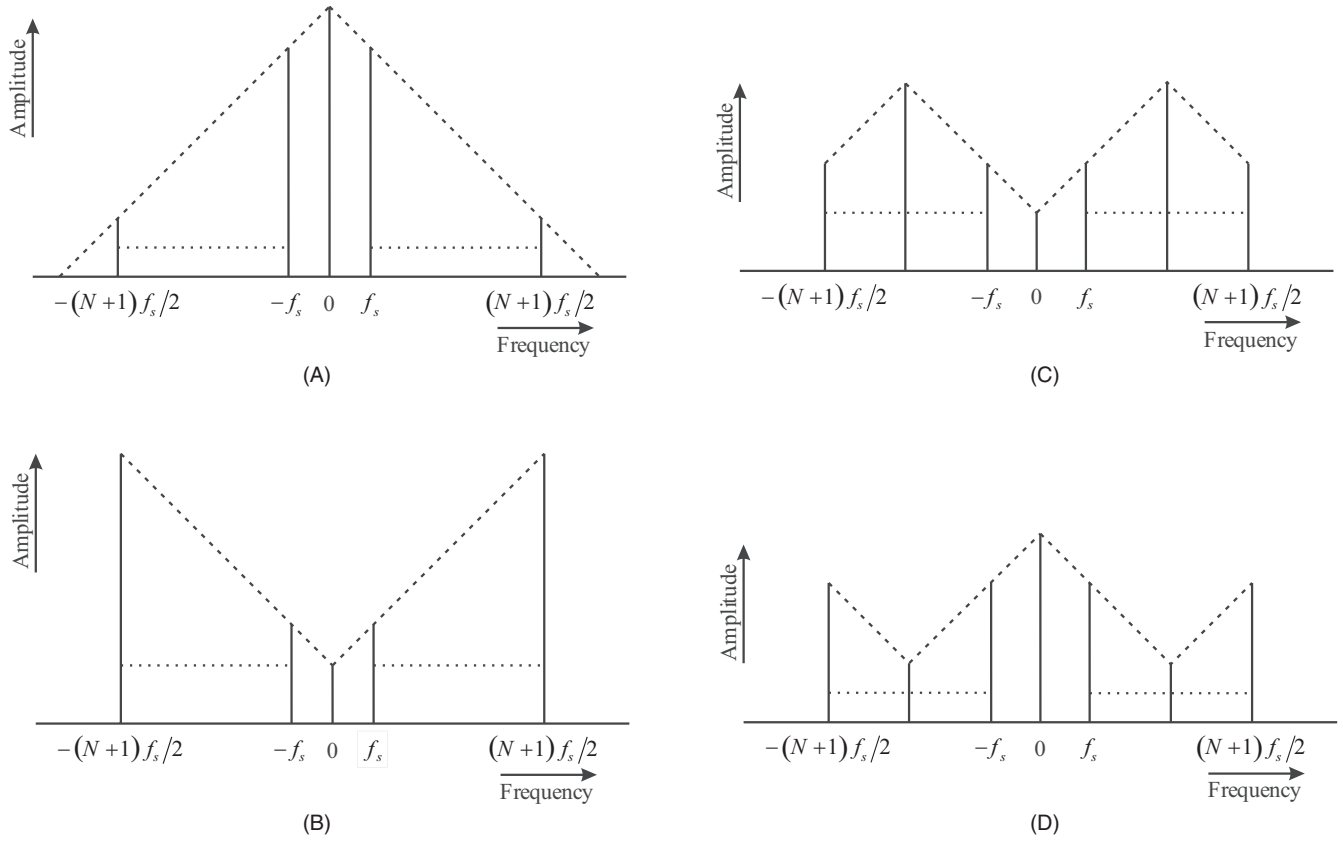

FIGURE 7 (A) Hill pattern, (B) Valley pattern, (C) M pattern, and (D) W pattern

Table 4 presents the results for MCPC signals developed based on raised cosine patterns. The same sequence ordering of 12 345 was selected for this table. One can see that no improvements in terms of PMEPR or sidelobe levels are obtained when using Hamming, Hanning, or Blackman window coefficients as the subcarrier weights for MCPC signals. However, desirable results are obtained using Kaiser window coefficients with β varying from 0.3 to 1.5.

5 | DIFFERENTIAL GEOMETRIC PROGRESSION (DGP) WEIGHTING

In this section, we present a novel technique for developing MCPC signals based on a DGP weighting approach. The weighting coefficients are obtained based on the concept of a hill pattern discussed in Section 4. Figure 8 presents the weighting factors developed using the DGP method based on favorable results obtained from the hill pattern. This combination of the hill pattern and GP defines the concept

TABLE 3 Experimental results of pattern-based weighting for 5×5 MCPC signals for the sequence ordering 12 345

Pattern	w_1	w_2	w_3	w_4	w_5	SL (dB)	PMEPR
Hill	0.1	0.9	1.0	0.9	0.1	20.50	2.5176
Valley	1.0	0.9	0.1	0.9	1.0	5.747	2.4408
M	0.1	1.0	0.7	1.0	0.1	10.35	3.1058
W	1.0	0.1	0.7	0.1	1.0	6.515	2.6913

TABLE 4 Results of subcarrier weighting using window coefficients for a 5×5 MCPC signal for the sequence ordering 12 345

Window	SL (dB)	PMEPR
Hamming	12.39	2.0687
Hanning	12.90	2.2392
Blackman	12.71	2.0687
Kaiser ($\beta = 0.1$)	13.74	2.0814
Kaiser ($\beta = 0.2$)	14.44	1.7299
Kaiser ($\beta = 0.3$)	14.45	1.7261
Kaiser ($\beta = 0.4$)	14.42	1.7199
Kaiser ($\beta = 0.5$)	14.40	1.7124
Kaiser ($\beta = 0.6$)	14.37	1.7031
Kaiser ($\beta = 0.7$)	14.33	1.6917
Kaiser ($\beta = 0.8$)	14.26	1.6781
Kaiser ($\beta = 0.9$)	14.24	1.6624
Kaiser ($\beta = 1.0$)	14.17	1.6446
Kaiser ($\beta = 1.5$	13.89	1.6247
Kaiser ($\beta = 2$)	13.53	1.5739
Kaiser ($\beta = 2.5$)	13.43	1.7756

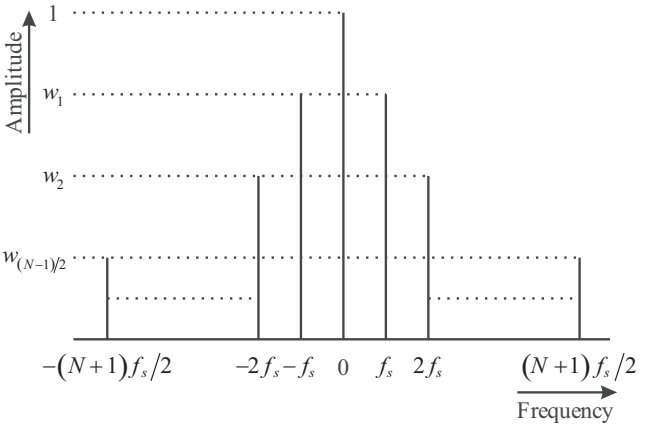

FIGURE 8 DGP weighting

of DGP weighting. The differences between consecutive weights always follow a GP (ie, $(1-w_1), (w_1-w_2), \ldots, (w_{N+1/2-1}-w_{N+1/2})$ represent a geometric progression). The slope of the line joining the tips of two adjacent subcarrier frequencies increases according to a GP on either side of the zero frequency. As the number of subcarriers increases, this pattern approaches a raised cosine pattern.

Consider an MCPC signal with N chips and N subcarriers by setting $N = 5$. In this case, a 5×5 MCPC signal is developed with subcarrier frequencies of $-2f_s$, $-f_s$, 0, f_s, and $2f_s$ and allocated with weights of m, n, 1, n, and m, respectively. Here, m and n are selected such that $m < n < 1$. The corresponding frequency representation is presented in Figure 9A, where the factor b represents the common ratio. The resulting weights are defined in (5).

$$n - m = b(1-n),$$

$$n - m = b - bn,$$

$$n(1+b) = b + m,$$

$$n = \frac{b+m}{1+b}. \tag{5}$$

Similarly, an MCPC signal was developed for seven subcarriers. Therefore, a 7×7 MCPC signal with subcarrier frequencies of $-3f_s, -2f_s, -f_s, 0, f_s, 2f_s$, and $3f_s$ was given weights m, n, p, 1, p, n, and m, respectively, such that $m < n < p < 1$. The resulting frequency representation is presented in Figure 9(B). The derived weights are defined in (6) and (7).

$$p - n = b(1-p),$$

$$n - m = b^2(1-p) = b(p-n),$$

$$p = \frac{n+p}{1+b},$$

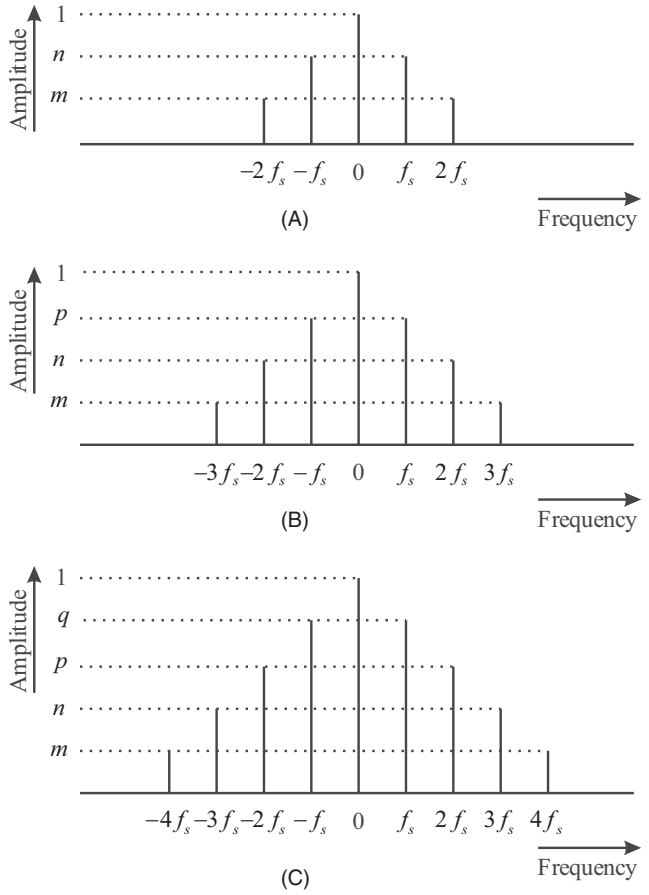

FIGURE 9 (A) DGP weighting for a 5×5 MCPC signal, (B) DGP weighting for a 7×7 MCPC signal, and (C) DGP weighting for a 9×9 MCPC signal

$$n - m = b(p - n),$$

$$n = \frac{bp + m}{1 + b},$$

$$n = \frac{b\left(\frac{n+b}{1+b}\right) + m}{1 + b},$$

$$n = \frac{b^2 + (1+b)m}{(1+b)^2 - b}, \tag{6}$$

$$p = \frac{\frac{b^2+(1+b)m}{(1+b)^2-b} + b}{(1+b)},$$

$$p = \frac{m + b(1+b)}{(1+b)^2 - b}. \tag{7}$$

Finally, for nine subcarriers, a corresponding 9×9 MCPC signal with subcarrier frequencies of $-4f_s, -3f_s, -2f_s, -f_s, 0, f_s, 2f_s, 3f_s$, and $4f_s$ was assigned weights $m, n, p, q, 1, q, p, n$, and m, respectively, such that $m < n < p < q < 1$. The corresponding frequency representation is presented in Figure 9C. The derived weights are defined in (8), (9), and (10).

$$(q - p) = b(1 - q),$$

$$(p - n) = b^2(1 - q)\, b(q - p),$$

$$(n - m) = b^3(1 - q) = b(p - n),$$

$$q - p = b - bq,$$

$$q = \frac{b + p}{1 + b},$$

$$p - n = b(q - p),$$

$$n = (1 + b)p - bq,$$

$$n = (1 + b)p - b\left(\frac{b + p}{1 + p}\right),$$

$$n = \frac{\left[(1+b)^2 - b\right]p - b^2}{1 + b},$$

$$n - m = b(p - n),$$

$$n = \frac{bp + m}{1 + b},$$

$$p = \frac{m + b^2}{(1+m)^2 - 2b}, \tag{8}$$

$$q = \frac{\left(m + b^2\right) + b\left[(1+b)^2 - 2b\right]}{(1+b)\left[(1+b)^2 - 2b\right]}, \tag{9}$$

$$\frac{n - m}{p - n} = b,$$

$$(1 + b)n - m = bp,$$

$$(1 + b)n - m = b\left(\frac{m + b^2}{(1+m)^2 - 2b}\right),$$

$$n = \frac{m\left[(1+b)^2 - b\right] + b^3}{(1+b)\left[(1+b)^2 - 2b\right]}. \tag{10}$$

We defined equations for MCPC signals with five, seven, and nine subcarriers. The relationships between each weighting coefficient for various MCPC lengths are defined as follows:

$$5\times 5: n = \frac{b+m}{1+b} \text{ where } m < n < 1 \ ,$$

$$7\times 7: n = \frac{b^2 + (1+b)\ m}{\left(1+b^2\right) - b} \ ,$$

$$p = \frac{m+b(1+b)}{\left(1+b^2\right)-b} \text{ where } m < n < p < 1,$$

$$9\times 9: n = \frac{m\left[(1+b)^2 - b\right] + b^3}{(1+b)\left[(1+b)^2 - 2b\right]},$$

$$p = \frac{m+b^2}{(1+b)^2 - 2b},$$

$$q = \frac{\left(m+b^2\right) + b\left[(1+b)^2 - 2b\right]}{(1+b)\left[(1+b)^2 - 2b\right]},$$

where $m < n < p < q < 1$.

Here, m, n, p, and q are weighting coefficients and the factor b represents the common ratio.

For the 5×5 MCPC signal, the weights are defined in (5), where m is considered an independent variable. By varying the value of m from 0.1 to 0.9, several ordered pairs (m, n) are generated. Based on the results, it is evident that a reduction in the sidelobe level is possible for all values of m. However, our analysis indicates that as the sidelobe level decreases, the PMEPR level increases significantly for certain ordered pairs of (m, n) in the range of $0.1 \le m \le 0.4$. For m values ranging from 0.5 to 0.9, both PMEPR and sidelobe levels are reduced, as shown in Table 5. Therefore, this range is more favorable for the simultaneous reduction of sidelobes and PMEPR. For a 7×7 MCPC signal, the weights are defined in (6) and (7). In this case, favorable results are obtained in the range of $0.4 \le m \le 0.8$, as shown in Table 6. For a 9×9 MCPC signal, the weights are defined in (8), (9), and (10). In this case, desirable results are obtained for the full range of m from 0.1 to 0.9, as shown in Table 7. As the common ratio b increases, improvements in terms of PMEPR and sidelobe level reduction can be observed for an increased range of m. Figure 10A presents an autocorrelation plot for a 5×5 MCPC signal developed using the DGP method for the sequence ordering 12 345 by choosing the factor $m = 0.6$. Similarly, Figure 10B presents an autocorrelation plot of a 7×7 MCPC signal developed using the DGP method for the sequence ordering 1 234 567 by choosing the factor $m = 0.5$.

TABLE 5 Experimental results for a 5×5 MCPC signal with the ordering 12 345 and $b = 2$

m	SL (dB)	PMEPR
P4 based	13.80	1.7200
0.1	25.18	2.3845
0.2	26.88	2.1685
0.3	25.10	1.9752
0.4	24.21	1.8090
0.5	23.47	1.6706
0.6	23.62	1.5586
0.7	21.14	1.5984
0.8	18.08	1.6479
0.9	15.73	1.6932

TABLE 6 Experimental results for a 7×7 MCPC signal with the ordering 1 234 567 and $b = 2$

m	SL (dB)	PMEPR
P4 based	12.80	1.9300
0.1	17.97	2.4117
0.2	18.61	2.1140
0.3	19.14	1.9469
0.4	19.66	1.9084
0.5	19.65	1.9067
0.6	18.58	1.9135
0.7	17.02	1.9208
0.8	15.49	1.9259
0.9	14.14	1.9280

TABLE 7 Experimental results for a 9×9 MCPC signal with the ordering 123 456 789 and $b = 2$

m	SL (dB)	PMEPR
P4 based	12.80	7.3000
0.1	22.38	5.6147
0.2	21.76	5.9247
0.3	21.24	6.2100
0.4	20.72	6.5560
0.5	19.94	6.6676
0.6	18.82	6.8479
0.7	17.53	6.9990
0.8	16.35	7.1238

6 | COMPARISON AND ANALYSIS OF VARIOUS SIDELOBE REDUCTION METHODS

A lower PMEPR level is desirable for the reliable operation of linear power amplifiers. Lower sidelobe levels are essential for improving the detection capabilities of radar. MCPC signals provide many advantages, such as protection against jamming and clutter, but PMEPR and sidelobe levels represent significant obstacles to their successful implementation. Therefore, to leverage the favorable features of MCPC signals, the reduction of sidelobe levels is crucial.

A TSSWA can be used at the receiving end to precisely distinguish the mainlobe from sidelobes. This involves the

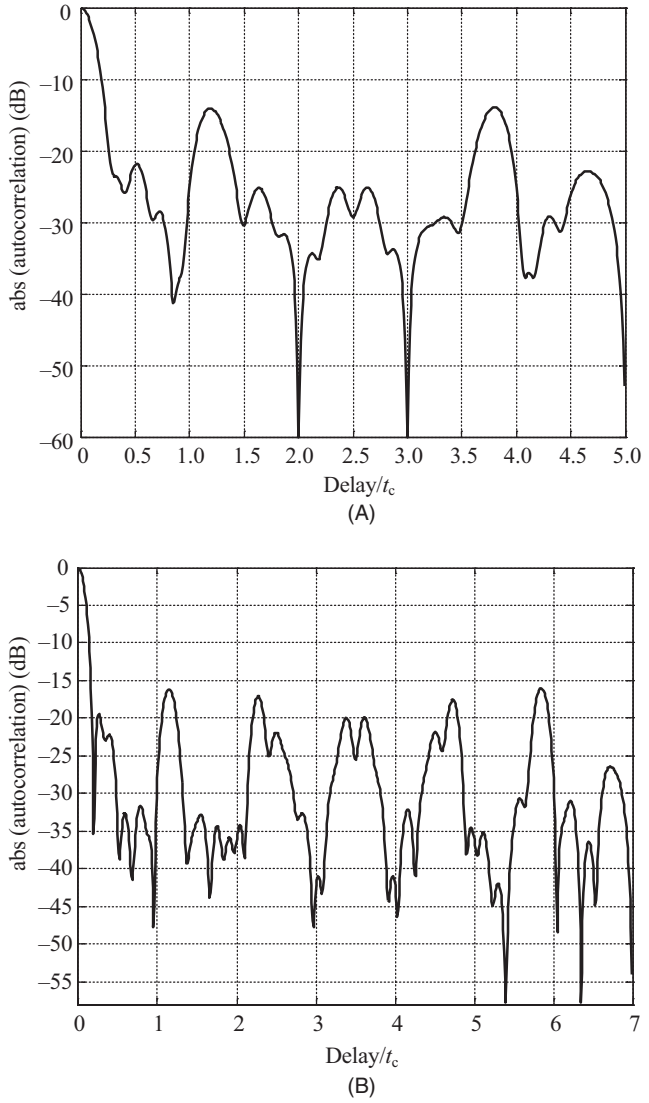

FIGURE 10 (A) Autocorrelation of DGP based on a 5×5 MCPC signal and (B) Autocorrelation of DGP based on a 7×7 MCPC signal

direct manipulation of autocorrelation without disturbing the original signal. However, subcarrier weighting involves changing the weights of subcarriers. DSW yields desirable results for random values of maximum-to-minimum-weight ratios. However, favorable ratios are not deterministic because frequency symmetry around the zero frequency is not maintained.

PBSW involves the scaling of subcarriers by maintaining frequency symmetry in a particular shape. The weights that are used in this analysis follow a specific pattern. Desirable sidelobe reduction is evident when the differences in weights between the zero frequency subcarrier and adjacent subcarriers are small and the differences in weights between the zero frequency subcarrier and furthest subcarriers are large. PMEPR reduction cannot be associated with a reduction in sidelobe levels because weights are picked randomly. Negative weights result in sidelobe reduction but significantly increase the PMEPR. The best PMEPR was obtained for a hill-pattern-based MCPC signal. This motivated us to perform additional experiments using raised cosine windows. A Kaiser window with particular values of β yielded the most favorable results. The potential for sidelobe reduction using a hill pattern and Kaiser window motivated us to consider a weighting scheme based on the DGP method. For certain ranges of weights, it is possible to obtain a joint reduction of PMEPR and sidelobe levels. In a DGP-based 7×7 MCPC signal with an ordering of 1 234 567, an improvement of 4.22 dB was observed in the PMEPR level compared with a P4-based MCPC signal.

7 | CONCLUSION

In this paper, we proposed novel subcarrier weighting techniques to develop MCPC signals. Various methods were employed to reduce PMEPR and sidelobe levels. First, the TSSWA method was used for reducing the sidelobe levels of MCPC signals. However, the envelope of a signal cannot be manipulated using this approach. Therefore, significant improvements in the PMEPR level were not observed based on the TSSWA method. Hill-pattern-based weighting results in superior reduction in sidelobe levels. In this approach, a reduction in the sidelobe level was achieved, but no significant improvements in terms of the PMEPR level were achieved. When using Kaiser window coefficients as scaling factors, certain values of β resulted in the reduction of both sidelobe and PMEPR levels. Additionally, the reduction of PMEPR and sidelobe levels was achieved using the DGP method.

ORCID

Channapatna Gopalkrishna Raghavendra https://orcid.org/0000-0002-0639-9695

REFERENCES

1. T. Hwang et al., *OFDM and its wireless applications: A survey*, IEEE Trans. Veh. Tech. **58** (2009), 1673–1694.
2. F. F. Kretschmer and B. L. Lewis, *Doppler properties of polyphase coded pulse compression waveforms*, IEEE Trans. AES **19** (1983), 521–531.
3. N. Levanon, *Multifrequency complementary phase coded radar signal*, IEE Proc.-Radar, Sonar Navig. **147** (2000), 276–284.
4. N. Levanon, Multifrequency signal structure for radar systems, US Patent, no. 6, 392,588, May 2002.
5. C. Ni, Y. Ma, and T. Jiang, *A novel adaptive tone reservation scheme for PAPR reduction in large scale multi-user MIMO-OFDM systems*, IEEE Wirel. Commun. Lett. **5** (2016), 480–483.
6. H. Li, T. Jiang, and Y. Zhou, *An improved tone reservation scheme with fast convergence for PAPR reduction in OFDM systems*, IEEE Trans. Broad. **57** (2011), 902–906.
7. J. Wang, X. Lv, and W. Wu, *SCR-based tone reservation schemes with fast convergence for PAPR reduction in OFDM system*, IEEE Wirel. Commun. Lett. **8** (2019), 624–627.

8. E. Mozeson and N. Levanon, *Multicarrier radar signals with low peak-to-mean envelope power ratio*, IEE Proc.-Radar Sonar Navig. **150** (2003), no. 2, 71–77.
9. T. Huang and T. Zhao, *Low PMEPR OFDM radar waveform design using the iterative least squares algorithm*, IEEE Signal Process. Lett. **22** (2015), 1975–1979.
10. G. Lellouch, A. K. Mishra, and M. Inggs, *Design of OFDM radar pulses using genetic algorithm based techniques*, IEEE Trans. Aerospace Electron. Syst. **52** (2016), 953–1965.
11. C. G. Raghavendra et al., *A novel approach to reduce the PMEPR of MCPC signal using random phase algorithm*, Informacije MIDEM, J. Microelectron., Electron. Compon. Materials **48** (2018), 63–70.
12. D. Li, X. Dai, and H. Zhang, *Sidelobe suppression in NC-OFDM systems using constellation adjustment*, IEEE Commun. Lett. **13** (2009), 327–329.
13. H. Li et al., *Orthogonal frequency division multiplexing linear frequency modulation signal design with optimised pulse compression property of spatial synthesised signals*, IET Radar Sonar Navig. **10** (2016), 1319–1326.
14. T. Bai, N. Zheng, and S. Chen, *OFDM MIMO radar waveform design for targets identification*, ETRI J. **40** (2018), 592–603.
15. C. Ni, T. Jiang, and W. Peng, *Joint PAPR reduction sidelobe suppression using signal cancellation in NC-OFDM based cognitive radio systems*, IEEE Trans. Veh. Tech. **64** (2015), 964–972.
16. A. Tom, A. Sahin, and H. Arslan, *Suppressing alignment: Joint PAPR and out-of-band power leakage reduction for OFDM based systems*, IEEE Trans. Commun. **64** (2016), 1100–1109.
17. N. A. Sivadas and S. M. Sameer, *Joint technique for sidelobe suppression and peak-to-average power ratio reduction in non-contiguous OFDM-based cognitive radio networks*, Int. J. Electron. **104** (2016), 190–203.
18. C. G. Raghavendra et al., *Joint reduction of PMEPR and sidelobe in multicarrier radar signals using ZC and SC method*, WSEAS Trans. Commun. **19** (2020), 9–17.
19. B. L. Lewis, *Range-time-sidelobe reduction technique for FM-derived polyphase PC codes*, IEEE Trans. Aerospace Electron. Syst. **29** (1993), 834–840.
20. R. Sato and M. Shinriki, *Time sidelobe reduction technique for binary phase coded pulse compression*, in Proc. IEEE Int. Radar Conf. (Alexandria, VA, USA), May 2000, pp. 809–814.
21. R. Sato, I. Sasase, and M. Shinriki, *Time sidelobe reduction technique with small S/N loss for binary-coded pulse compression*, in Proc. CIE Int. Conf. Radar (Beijing, China), Oct. 2001, pp. 947–951.
22. I. Cosovic, S. Brandes, and M. Schnell, *Subcarrier weighting: A method for sidelobe suppression in OFDM systems*, IEEE Commun. Lett. **10** (2006), 444–446.

AUTHOR BIOGRAPHIES

Channapatna Gopalkrishna Raghavendra obtained his BE degree, MTech degree, and PhD in Electronics and Communication in 2001, 2004, and 2018, respectively. He worked as an engineer for the Aeronautical Development Agency (ADA, Ministry of Defence, Govt. of India) from 2001 to 2002.He has worked as an associate professor at the department of Electronics and Communication, Ramaiah Institute of Technology, Bangalore, India from 2004. He has over 16 years of teaching experience. He is a principal investigator for several projects funded by the VGST, Govt. of Karnataka, IEEE-Bangalore section, IETE-Bangalore Center, and KSCST, Bangalore. He has filed several Indian patents in the area of signal processing. He has published papers in several international journals. He is a Fellow of IETE, Senior Member of IEEE, and Member of IEI, IMAPS, and ISTE.

Raghu Srivatsa Marasandra Prakash received his BE degree in Electronics and Communication Engineering from the Ramaiah Institute of Technology, Bangalore, India in 2017. From 2017 to 2019, he worked for Rolls-Royce. Since 2019, he has worked for Boeing as a software engineer. His main research interests are radar signal processing and avionics.

Vignesh Nayak Panemangalore received his BE degree in Electronics and Communication from the Ramaiah Institute of Technology, Bangalore, India in 2017. Since 2017, he has worked with Infosys Ltd. as a software engineer. His main research interests are radar signal processing and digital communication.